ORIGINAL RESEARCH

Bagcilar Med Bull 2022;7(1):12-19
DOI: 10.4274/BMB.galenos.2021.2021-11-120

A Retrospective Analysis of the Most Common Bone Metastases of Various Malignant Tumors with Cross-sectional Imaging and 18-FDG-PET/CT Data

Kesitsel Görüntüleme ve 18-FDG-PET BT Verileri ile Çeşitli Malign Tümörlerin En Sık Görülen Kemik Metastazlarının Retrospektif Analizi

Mehmet Öncü[1], Deniz Özel[2]

[1]University of Health Sciences Turkey, İstanbul Bağcılar Training and Research Hospital, Clinic of Radiology, İstanbul, Turkey
[2]University of Health Sciences Turkey, Bakırçay University Çiğli Training and Research Hospital, Clinic of Radiology, İzmir, Turkey

Abstract

Objective: To evaluate bone metastases quantitatively and qualitatively with cross-sectional imaging and fluor-18 fluorodeoxyglucose-positron emission tomography (18-FDG-PET) computed tomograph (CT) data.

Method: To obtain study data, the archive of the nuclear medicine of our institute was retrospectively searched for the period from January 2015 to December 2018. For magnetic resonance imaging (MRI) evaluation, the signal intensity ratio of involved tissue to normal adjacent tissue was chosen. For CT evaluation, metastases were labelled to be lytic or sclerotic with regard to the mean density values. Finally, the maximum and the mean standardized uptake values and metabolic tumor volume values were evaluated quantitatively.

Results: All bone metastases presented hypointensity on T1 sequences whereas 96.4% of them presented hypointensity on T2 and hyperintensity on short tau inversion recovery (STIR) sequences. STIR images were found to be valuable to detect metastases. 18-FDG-PET/CT metabolic tumor volume values showed statistically significant difference with regard to the metastatic tumor types. There was not a statistically significant difference between 18-FDG-PET/CT parameters of lytic and sclerotic metastases.

Conclusion: We recommend performing STIR images in routine protocol being performed for other reasons such as disc pathologies to detect incidental bone metastases. MRI signal intensity and SUV values cannot be used to predict the tumor histopathology. Sclerotic or lytic appearance does not correlate 18-FDG-PET/CT parameters for breast and SUV_{max} values for lung cancers. Metabolic tumor volume values differ with the primary tumor histopathology and are also defined to be a promising prognostic factor in the future.

Keywords: 18-FDG-PET/CT, bone metastases, CT, MRI

Öz

Amaç: Kesit görüntüleme ve flor-18 florodeoksiglikoz-pozitron emisyon tomografi (18-FDG-PET) bilgisayarlı tomografi (BT) verileri ile kemik metastazlarını kantitatif ve kalitatif olarak değerlendirmektir.

Yöntem: Çalışma verilerini elde etmek için, enstitümüzün nükleer tıp arşivi, Ocak 2015-Aralık 2018 arasındaki dönem için geriye dönük olarak araştırıldı. Manyetik rezonans görüntüleme (MRG) değerlendirmesi için ilgili dokunun normal bitişik dokuya sinyal yoğunluğu oranı seçildi. BT değerlendirmesi için, ortalama yoğunluk değerlerine göre metastazlar litik veya sklerotik olarak tanımlandı. Son olarak, 18-FDG-PET BT'de maksimum ve ortalama standart uptake değerleri ve metabolik tümör hacmi değerleri kantitatif olarak değerlendirildi.

Bulgular: Tüm kemik metastazları T1 sekanslarında hipointens iken, %96,4'ü T2'de hipo ve kısa tau inversiyon kurtarma (STIR) sekanslarında hiperintensite göstermiştir. STIR görüntüleri metastazı saptamada daha etkin bulundu. Çeşitli tümör tipleri arasında istatistiksel olarak anlamlı bir MRG sinyal yoğunluğu farkı yoktu. 18-FDG-PET/BT metabolik tümör hacmi değerleri metastatik tümör tiplerine göre istatistiksel olarak anlamlı fark gösterdi. Litik ve sklerotik metastazların 18-FDG-PET/BT parametreleri arasında istatistiksel olarak anlamlı bir fark yoktu.

Sonuç: Rastlantısal kemik metastazlarını saptamak için disk patolojileri gibi diğer nedenlerle rutin protokolde STIR görüntülerinin yapılmasını öneriyoruz. MRG sinyal yoğunluğu ve SUV değerleri, tümör histopatolojisini tahmin etmek için kullanılamaz. Meme kanseri metastazları için sklerotik veya litik görünüm 18-FDG-PET/BT parametrelerini ve akciğer kanserleri için SUV_{maks} değerlerini etkilemez. Metabolik tümör hacim değerleri, bazı yeni makalelerde belirtildiği gibi prognostik faktör olarak tanımlanabilir.

Anahtar kelimeler: 18-FDG-PET/BT, BT, kemik metastazları, MRG

Address for Correspondence: Deniz Özel, University of Health Sciences Turkey, Bakırçay University Çiğli Training and Research Hospital, Clinic of Radiology, İzmir, Turkey
E-mail: denizozel34@hotmail.com **ORCID:** orcid.org/0000-0002-4950-001X **Received:** 25.11.2021 **Accepted:** 29.12.2021

Cite this article as: : Öncü M, Özel D. A Retrospective Analysis of the Most Common Bone Metastases of Various Malignant Tumors with Cross-sectional Imaging and 18-FDG-PET/CT Data. Bagcilar Med Bull 2022;7(1):12-19

Introduction

The skeletal system is one of the three most occupied regions by the metastases of malignant tumors following the lung and the liver. The presence of bone metastases may be the first evidence while the primary tumor is yet unknown. Defining additional metastases will change the treatment options for cancer patients. In nuclear imaging, fluor-18 fluorodeoxyglucose-positron emission tomography (18-FDG-PET) computed tomography (CT) is an accurate technique "for the detection of skeletal metastases and is superior to bone scan in several studies especially for osteoblastic metastases" (1,2). Considering the difficulties of obtaining pathological specimens, metastatic involvements are often evaluated with cross-sectional and nuclear medicine data. The aim of this study was to evaluate the bone metastatic involvement of various malignancies with cross- sectional and 18-FDG-PET/CT data.

Materials and Methods

The archive of the nuclear medicine clinic and the picture archiving and communication system (PACS) of our institute were retrospectively reviewed from January 2015 to December 2018. We chose the initial date when PACS got functional. This was a single-center study.

All magnetic resonance imaging (MRI) examinations were performed by means of a 1.5 Tesla superconducting magnet with high-speed gradients (Signa Excite, GE Medical Systems, Waukesha, Wisconsin, USA) with a dedicated coil.

Inclusion-exclusion criteria: Patients having malignant tumors with bone metastatic involvement were included in the study. All patients had at least one magnetic resonance (MR) and corresponding PET-CT images obtained after at least 1 month after chemotherapy and radiotherapy. The diagnoses were performed with biopsy results from the primary tumor or if possible, directly from the metastatic lesions.

For each MRI evaluation, two or three planar images were obtained, consisting of fat-suppressed short tau inversion recovery (STIR) images [TR/TE=2400-6280/50-70 ms, FOV=350-400×350-400 mm^2, matrix=192-320×192-240, slice thickness (ST)=4-6 mm, inversion time=170-220 ms], T1-weighted (TR/TE=240-718 ms/5-10 ms, FOV=280-400×280-400 mm^2, matrix=256×256, ST=4-6 mm), and T2-weighted images (TR/TE=1400-6640/80-120 ms, FOV=280-400×280-400 mm^2, matrix=256-330×256-252, ST=4-6 mm).

Nuclear medicine: The patients fasted for at least 6 hours and their blood glucose levels were measured immediately before the administration of FDG. All blood glucose levels were lower than 200 mg/dL. PET/CT images were acquired fifty to sixty minutes after the intravenous injection of 18F-FDG (5-6 MBq/kg body weight). All 18F-FDG PET/CT scans were obtained with a dedicated PET/CT scanner (Siemens Biograph 6, Chicago, IL, USA). After the initial low-dose CT (50 mAs, 140 kV, and 5-mm section thickness), PET images were acquired for 3 minutes per bed position in the 3-dimensional mode.

The FDG-PET/CT images were analyzed by an experienced nuclear medicine specialist using dedicated analysis software (Syngo.via, Siemens Healthcare, Knoxville, TN). The spherical volume of interest (VOI) was drawn to include metastatic bone lesion. Physiologic FDG uptakes of neighbor organs were not included in the VOI. Metabolic tumor volume (MTV) was defined as metastatic tumor volume with a standardized uptake value (SUV) threshold of 2.5. The SUV value was calculated as (the decay-corrected activity of tissue volume)/(injected activity/body mass). MTV, the maximum value of SUV (SUV_{max}) and the mean of SUV (SUV_{mean}) were automatically calculated.

Cross-sectional evaluating: Signal intensity ratios were evaluated by the same experienced radiologist with the PACS software in a largest possible region of interest. The target parameters were chosen to be T1, T2, STIR signal intensity of MRI. In MR imaging, the ratio of tumor-invaded bone marrow signal to the adjacent (nearest possible) non-occupied bone marrow signal was calculated for each parameter (For T1, T2 and STIR signals).

For the tumors with multiple foci, parameters were calculated for the largest lesion.

CT density values were used to define the metastatic involvement, as the groups of lytic and sclerotic with PET-CT images. If the mean density value of involved bone tissue was less than the mean density value of non-occupied bone tissue, this involvement was labelled as lytic and for the opposite situation they labelled as sclerotic. The metastases, showing both cystic and lytic components, were labelled with the dominant involvement.

Statistical Analysis

The power analysis was used to calculate the minimum patient data required for each comparison. Univariate variance analysis was used to compare signal intensity ratios for cross-sectional imaging and to compare 18-FDG-PET/CT parameters with regard to different malignancies with bone metastases. The Student's t-test was used to compare 18-FDG-PET/CT parameters for lytic and

sclerotic metastases for each malignancy. The chi-square test was employed for categorical comparisons namely in the evaluation of the distribution of lytic and sclerotic metastases. Microsoft Excel Program Version 1811 was used for storage and calculations. A p-value of less than 0.05 was considered to be significant.

Ethical approval: All procedures performed in the study involving human participants were in accordance with the ethical standards of the institutional and/or national research committee and with the 1964 Helsinki Declaration and its later amendments or comparable ethical standards. This study was approved by our IRB (date: 11.9.2018, no: 978). Informed consent was obtained from all individual participants included in the study.

Results

The total number of patients having malignant tumors with bone metastases was 225. One hundred thirty-eight (61.3%) of the patients were female and 87 (38,7 %) were male. The mean age of the patients was 57.1 years, ranging from 13 to 86 years. The distribution of the malignant tumors is shown in Table 1.

Table 1. The demographic data and the distribution of malignancies with bone metastases

Source of bone metastases	The mean age	Female (%)	No of patients	%
Breast	55.85	99.3	139	61.78
Lung	59.6	10.3	39	17.33
Prostate	70.2	0	12	5.33
Colon	60.2	58.3	11	4.88
Urinary bladder	59.4	60	5	2.22
Nasopharynx	40.5	0	4	1.78
Renal	63	0	3	1.34
Thyroid	56	33.3	3	1.34
Miscellaneous	53.8	22	9	4
Overall	57.2	61.3	225	100

All bone metastases presented hypointense on T1 images with the signal ratios between 0 and 1. The mean ratio was higher and closer to 1 for T2 images but there was not a statistically significant difference between the various tumor types. Most of the tumors (217 tumors and 96.4%) presented hyperintensity on STIR images and the mean signal ratio was greater than 1. There was not a statistically significant difference in various tumor types. The lytic-sclerotic distribution was different for each tumor metastases (Table 2). Figure 1 shows multiple breast cancer metastasis.

18-FDG-PET/CT SUV_{max} and SUV_{avg} values showed no statistically significant difference with regard to the tumor types except for MTV (Table 3). There were no statistically significant differences between PET-CT values of lytic and sclerotic metastases (Table 4). Figure 2 shows a breast cancer metastasis to the iliac bone with an MTV value of 16.8. Figure 3 shows increased detectability of the lesions with STIR image compared to T2 in a nasopharynx cancer case with multiple vertebral metastases. Figure 4 summarizes the cross-sectional image characteristics and PET-CT parameters of various bone metastases.

Discussion

The most common malignant tumor with bone metastases was breast cancer in our study. More than 60% of all patients had breast cancer. This tumor is commonly seen and tends to spread to bone tissues. According to our demographic data, the group with the highest mean age was the prostate, the lowest was the nasopharyngeal cancer cases. Metastatic breast cancer was seen nearly always among females (except 1 case). Metastatic lung cancer was mostly seen among males.

After obtaining CT density values, all prostate metastases were defined to be sclerotic. There was a balance for the lung metastases. Breast and colon metastases showed sclerotic predominance. Our results were concordant with

Table 2. Signal intensity ratios for CT and MRI. Data presented as mean ± standard deviation and range in brackets [F=0.88 (T1), 2.36 (T2), 0.04 (STIR)] (chi-square: 11.57)

Source of bone metastases	T1 (Mean ± SD)	T2 (Mean ± SD)	STIR (Mean ± SD)	Lytic metastases predominance (%)
Breast (n=139)	0.43±0.14 (0.2-0.81)	0.57±0.18 (0.3-1)	2.5±2.14 (0.33-15)	38.1
Lung (n=39)	0.47±0.17 (0.2-0.9)	0.68±0.26 (0.23-1)	2.61±0.87 (1.2-4.8)	51.3
Prostate (n=12)	0.4±0.11 (0.3-0.6)	0.67±0.09 (0.6-0.7)	2.56±0.9 (1.4-4.6)	0
Colorectal (n=11)	0.47±0.15 (0.3-0.7)	0.68±0.12 (0.6-0.81)	2.3±1.24 (1.2-3.9)	27.2
p	0.42	0.09	0.99	<0.01

SD: Standard deviation, CT: Computed tomography, MRI: Magnetic resonance imaging, STIR: Short tau inversion recovery

Table 3. Comparison of nuclear medicine parameters regards to different malignancies with bone metastases. Data presented as mean ± standard deviation and range in brackets (other metastatic tumors were not included in the statistical evaluation because the number of cases was not sufficient)
[F=2.53 (SUV_{max}), 2.36 (SUV_{avg}), 3.85 (MTV)]

Source of bone metastases	SUV_{max} (Mean ± SD)	SUV_{avg} (Mean ± SD)	MTV (Mean ± SD)
Breast cancer (n=139)	10.18±5.17 (2.63-22.83)	5.01±1.3 (0.05-8.05)	16.2±20.1 (0.05-108)
Lung cancer (n=39)	14.85±11.04 (5.46-60.23)	6.15±2.1 (3.59-17.37)	45.7±37.3 (0.99-264.5)
Prostate cancer (n=12)	8.58±10.4 (5.62-13.56)	4.57±2.04 (3.96-5.37)	39.3±38.6 (3.37-117.5)
Colorectal cancer (n=11)	9.27±9.52 (3.99-13.15)	4.7±1.96 (3.18-5.94)	55.4±39.2 (4.61-141.77)
p	0.32	0.29	<0.01

SUV: Standardized uptake value, SD: Standard deviation, MTV: Metabolic tumor volume

Table 4. Comparing nuclear medicine parameters for lytic and sclerotic metastases for each malignancy. Data presented as mean ± standard deviation

	SUV_{max} (Mean ± SD)	SUV_{avg} (Mean ± SD)	MTV (Mean ± SD)	p
Lytic breast cancer metastases (n=53)	10.22±4.97	4.86±1.45	20±14.54	SUV_{max}: NA
Sclerotic breast cancer metastases (n=86)	10.99±5.04	5.17±1.37	13.1±13.94	SUV_{avg}: NA MTV: 0.10
Lytic lung cancer metastases (n=20)	19.1±8.37	7.16±4.34	20.02±55.43	SUV_{max}: 0.07
Sclerotic lung cancer metastases (n=19)	12.03±5	5.36±3.45	13.16±50.13	SUV_{avg}: NA MTV: NA
Lytic colorectal cancer metastases (n=3)	11±2.55	5.35±2.58	80.7±30.8	SUV_{max}: NA
Sclerotic colorectal cancer metastases (n=8)	9.28±1.91	4.63±2.88	50.4±35.3	SUV_{avg}: NA MTV: NA

NA: Not applicable due to power analysis, SD: Standard deviation, SUV: Standardized uptake value, MTV: Metabolic tumor volume

Figure 1. Shows multiple breast cancer metastasis

a review article (3). That was the only semi-quantitative parameter we evaluated in this study. The bone densities show large variability for each patient and it seems to be impossible to standardize them because can be affected by many parameters such as, age, gender, drug use etc. So, we grouped bone metastases as lytic and sclerotic. With this study, SUV and MTV values were also compared to evaluate if these values could be affected in terms of lytic and sclerotic metastases for different malignancies.

There was not a statistically significant difference between SUV values of lytic and sclerotic metastases. We must remind the readers about the limited data for many different cancer metastases at this point. The number of cases allowed to evaluate two kinds of tumor's metastatic lesions. They were breast and lung cancer metastases. Our results were concordant with an article and the authors declared that PET with 18F-fluoride showed no differences in "the uptake of 18F between lytic and sclerotic lesions for breast cancer metastases" and the substance used in this study was also different (4). Likewise, Koolen et al. (5) reported 4 cases of FDG-avid sclerotic bone metastases in breast cancer patients.

Choosing the quantitative parameters for MRI was important from the very beginning of the study. The signal intensity of the tissue alone would not be an optimal choice because the signal intensity of bone marrow can be affected by several issues such as red-yellow marrow distribution

Figure 2. Shows a breast cancer metastasis to the iliac bone with a MTV value of 16.8

MTV: Metabolic tumor volume, CT: Computed tomography, PET: Positron emission tomography

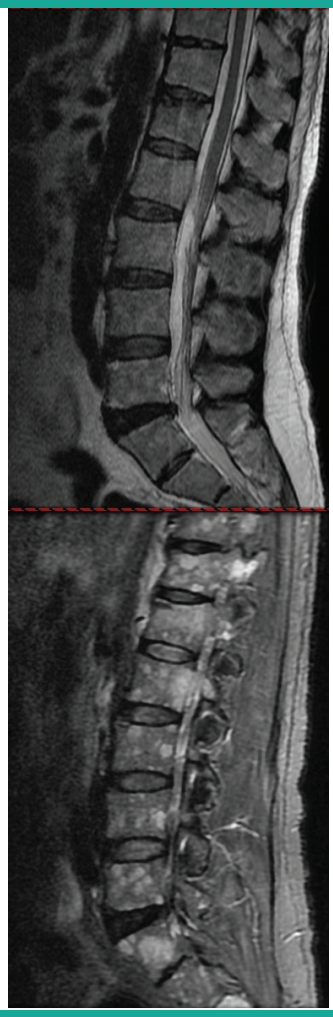

Figure 3. Shows increased detectability of the lesions with STIR image compared with T2 in a nasopharynx cancer case with multiple vertebral metastases

STIR: Short tau inversion recovery

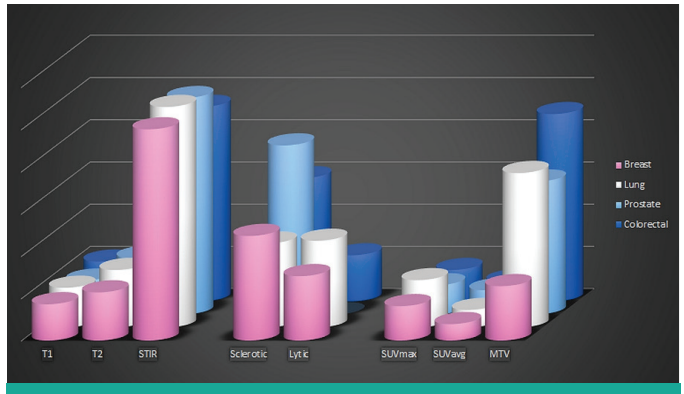

Figure 4. The chart summarizes the cross-sectional image characteristics and PET-CT parameters of various bone metastases

PET-CT: Positron emission tomography-computed tomography, SUV: Standardized uptake value, MTV: Metabolic tumor volume, STIR: Short tau inversion recovery

or hemopoietic diseases such as anemia. We experienced that even the patient's weight might affect alone the signal intensity. We decided to use the lesion intensity ratio to nearby non-occupied tissue intensity ratio to standardize the results.

In evaluating T1 signal intensity, all ratio values were between 0 and 1, which indicates that all bone metastases were hypointense on T1 images. It can be justified that T1 hyperintensity can exclude metastasis alone. On the other hand, we must note that we encountered only one patient with bone metastases from malignant melanoma and melanin was a known T1 hyperintense substance. However, this patient's metastases also showed T1 hypointensity.

According to our results, most of the bone metastases showed hyperintensity on STIR images and the mean STIR intensity was higher than 1 for bone metastases. On the other hand, the mean T2 signal intensity was higher than the mean T1 signal intensity and was closer to 1, which indicates that bone metastases were hypointense as they were on T1 images most of the time (93%) 4.6% of the bone metastases the ratio was 1 indicates bone metastases were completely invisible on T2 sections. As a well-known entity, one of the most important factors for a lesion to be detected is its contrast with the adjacent or normal identical tissues. According to our results, the presence of T2 images cannot make a real contribution to existing parameters in order to define metastatic involvement. Instead, STIR sequences are potentially more applicable to detect them. In spinal MRI imaging, T2 sequences are obtained in a routine manner (for instance, degenerative disc pathologies). Here, we recommend obtaining both T2 and STIR images together in routine examinations to detect incidental metastasis of the patients being examined for the other reasons. As mentioned in the introduction, the presence of bone metastases may be the first evidence while the primary tumor is yet unknown. After a literature search, it was revealed that most of the studies were concerning about detectability of bone metastases for different modalities especially distinguishing bone metastases from the other lesions. Bratu et al. (6) concluded that bone metastases had no specific signal intensity. Velloni et al. (7) defined hepatocellular carcinoma metastases to be hyperintense on fat saturated images. A quantitative retrospective study was performed to distinguish lytic metastases from hemangiomas. Their parameters were T1 signal, chemical shift imaging, and diffusion-weighted imaging (8).

It was also planned to evaluate 18-FDG-PET/CT values qualitatively. For this purpose, SUV_{max} and SUV_{avg} values were examined. We did not find a statistically significant difference for both SUV_{max} and SUV_{avg} values for different tumor types. On the other hand, the mean MTV values were statistically different among tumor types. MTV represents the tissues showing active 18F-FDG uptake and consists of both the dual characteristics of volumetric data and the metabolic activity of the lesion (9). According to our results, colon cancer metastases showed the highest mean MTV values whereas breast cancer metastases showed the lowest. There are several studies mentioning the relationship between the mean MTV values and the prognostic outcome. First of them was a novel volume based on predictive values study promising prognostic indicators such as disease-free-survival. The parameters used in this study were MTV and total lesion glycolysis (10). Chung et al. (9) concluded that "MTV has a potential value in predicting short-term outcome and disease-free survival in patients with pharyngeal cancers". According to Ulaner et al. (11), "higher MTV values were associated with shorter overall survival for several different involvements (excluding bones)". They also concluded that "measures of FDG avidity are prognostic biomarkers in newly diagnosed metastatic bone cancers. SUV_{max} and TLG were both predictors of survival in breast cancer patients with bone metastases". There were two additional articles that mentioned MTV values to be used for clinical follow-up (12,13). It is necessary to remember that there are so many indicators to determine the disease's expected outcome, but MTV values may offer additional data.

According to recent studies, combining MRI and PET-CT values was found to be the most functional choice in evaluating bone metastases. There are many articles concerning the comparison of diagnostic performance for various PET-CT techniques. 18-FDG-PET/CT was defined as a superior technique for detecting bone metastases in several articles (14-17). Moreover, according to Avery and Kuo (18), "MRI and FDG-PET/CT outperformed CT in most situations. The diagnostic accuracy of X-ray and bone scintigraphy were notably inferior to other modalities". They performed a comparison among the five most common malignancies with bone metastases; they were lung cancer, breast cancer, multiple myeloma, lymphoma and prostate cancer with descending order. Furthermore, MRI was found to be better than other techniques on the per-patient and per-lesion basis for the diagnosis of vertebral metastases in another meta-analysis including 33 chosen studies (19). The radiologists tend to correlate imaging findings with SUV values before their final decision also vice versa for nuclear medicine specialists. In our case, we had the opportunity to discuss all cases in the multidisciplinary council.

When the subject is quantitative evaluation, we found an article which revealed quantitative signal parameters and compared healthy and metastatic tissues in terms of ADC values (20). This article was close to our subject but with the difference that we evaluated conventional T1, T2 signals.

Study Limitations

Contrast-enhanced slices were not standardized; some were obtained with gradient echo sequences and some were with spin echo sequences. Besides, contrast enhancement could be affected with other reasons such as the body weight,

administration process, and timing etc. Finally, some of the metastases were defined without contrast-enhanced slices. To obtain objective results, we felt ourselves to be forced to exclude contrast-enhanced images and this was the first limitation.

We could not include all tumor types in our study for statistical comparison because the total number of cases did not meet the requirements in power analysis. These tumors are grouped under the miscellaneous name. Our data were limited for different kinds of malignancies and this should be counted as the second limitation.

Conclusion

Obtaining STIR images to define incidental bone metastases in the routine protocol is recommended. The presence of an additional bone involvement of any malignancy will substantially change the outcome and intervening the therapy can positively affect the treatment. All bone metastases were T1 hypointense and STIR images were more applicable compared to T2 images. MRI signal intensity and SUV values cannot be used to distinguish the primary tumor. Sclerotic or lytic appearance does not affect 18-FDG-PET/CT parameters for breast and SUV_{max} values for lung cancers. MTV values differ with the primary tumor and that was assigned as a promising prognostic factor in recent studies.

Acknowledgement

We would like to thank nuclear medicine clinic for sharing their data.

Ethics

Ethics Committee Approval: All procedures performed in the study involving human participants were in accordance with the ethical standards of the institutional and/or national research committee and with the 1964 Helsinki Declaration and its later amendments or comparable ethical standards. This study was approved by our IRB (date: 11.9.2018, no: 978).

Informed Consent: Informed consent was obtained from all individual participants included in the study.

Peer-review: Externally peer-reviewed.

Authorship Contributions

Concept: M.Ö., D.Ö., Desing: M.Ö., D.Ö., Data Collection or Processing: M.Ö., D.Ö., Analysis or Interpretation: M.Ö., D.Ö., Drafting Manuscript: M.Ö., D.Ö., Final Approval and Accountability: M.Ö., D.Ö.

Conflict of Interest: No conflict of interest was declared by the authors.

Financial Disclosure: The authors declared that this study received no financial support.

References

1. Chang CY, Gill CM, Simeone FJ, Taneja AK, Huang AJ, Torriani M, et al. Comparison of the diagnostic accuracy of 99 m-Tc-MDP bone scintigraphy and 18 F-FDG PET/CT for the detection of skeletal metastases. Acta Radiol 2016;57(1):58-65.
2. Uchida K, Nakajima H, Miyazaki T, Tsuchida T, Hirai T, Sugita D, et al. (18)F-FDG PET/CT for Diagnosis of Osteosclerotic and Osteolytic Vertebral Metastatic Lesions: Comparison with Bone Scintigraphy. Asian Spine J 2013;7(2):96-103.
3. Macedo F, Ladeira K, Pinho F, Saraiva N, Bonito N, Pinto L, et al. Bone Metastases: An Overview. Oncol Rev 2017;11(1):321.
4. Petrén-Mallmin M, Andréasson I, Ljunggren O, Ahlström H, Bergh J, Antoni G, et al. Skeletal metastases from breast cancer: uptake of 18F-fluoride measured with positron emission tomography in correlation with CT. Skeletal Radiol 1998;27(2):72-76.
5. Koolen BB, Vegt E, Rutgers EJ, Wouter VV, Marcel P, Stokkel MP, et al. FDG-avid sclerotic bone metastases in breast cancer patients: a PET/CT case series. Ann Nucl Med 2012;26(1):86-91.
6. Bratu AM, Raica VP, Săcianu IA, Zaharia C, Popa VB, Lupu AR, et al. MRI differential diagnosis: bone metastases versus bone lesions due to malignant hemopathies. Rom J Morphol Embryol 2017;58(4):1217-1228.
7. Velloni F, Ramalho M, AlObaidy M, Matos AP, Altun E, Semelka RC. Bone Metastases of Hepatocellular Carcinoma: Appearance on MRI Using a Standard Abdominal Protocol. AJR Am J Roentgenol 2016;206(5):1003-1012.
8. Shi YJ, Li XT, Zhang XY, Liu YL, Tang L, Sun YS. Differential diagnosis of hemangiomas from spinal osteolytic metastases using 3.0 T MRI: comparison of T1-weighted imaging, chemical-shift imaging, diffusion-weighted and contrast-enhanced imaging. Oncotarget 2017;8(41):71095-71104.
9. Chung MK, Jeong HS, Park SG, Jang JY, Son YI, Choi JY, et al. Metabolic tumor volume of [18F]-fluorodeoxyglucose positron emission tomography/computed tomography predicts short-term outcome to radiotherapy with or without chemotherapy in pharyngeal cancer. Clin Cancer Res 2009;15(18):5861-5868.
10. Satoh Y, Onishi H, Nambu A, Araki T. Volume-based parameters measured by using FDG PET/CT in patients with stage I NSCLC treated with stereotactic body radiation therapy: prognostic value. Radiology 2014;270(1):275-278.
11. Ulaner GA, Eaton A, Morris PG, Lilienstein J, Jhaveri K, Patil S, et al. Prognostic value of quantitative fluorodeoxyglucose measurements in newly diagnosed metastatic breast cancer. Cancer Med 2013;2(5):725-733.
12. Kim YI, Kang HG, Kim SK, Kim JH, Kim HS. Clinical outcome prediction of percutaneous cementoplasty for metastatic bone tumor using (18)F-FDG PET-CT. Ann Nucl Med 2013;27(10):916-923.
13. Cysouw M, Bouman-Wammes E, Hoekstra O, Eertwegh AVD, Piet M, Moorselaar JV et al. Prognostic Value of [18F]-Fluoromethylcholine Positron Emission Tomography/Computed Tomography Before

Stereotactic Body Radiation Therapy for Oligometastatic Prostate Cancer. Int J Radiat Oncol Biol Phys 2018;101(2):406-410.

14. Capitanio S, Bongioanni F, Piccardo A, Campus C, Gonella R, Tixi L et al. Comparisons between glucose analogue 2-deoxy-2-(18F) fluoro-D-glucose and 18F-sodium fluoride positron emission tomography/computed tomography in breast cancer patients with bone lesions. World J Radiol 2016;8(2):200-209.

15. Seo HJ, Kim GM, Kim JH, Kang WJ, Choi HJ. 18F-FDG PET/CT in hepatocellular carcinoma: detection of bone metastasis and prediction of prognosis. Nuc Med Commun 2015;36(3):226-233.

16. Ito S, Kato K, Ikeda M, Iwano S, Makino N, Tadokoro M, et al. Comparison of 18F-FDG PET and bone scintigraphy in detection of bone metastases of thyroid cancer. J Nucl Med 2007;48(6):889-895.

17. Lange MB, Nielsen ML, Andersen JD, Lilholt HJ, Vyberg M, Petersen LJ. Diagnostic accuracy of imaging methods for the diagnosis of skeletal malignancies: A retrospective analysis against a pathology-proven reference. Eur J Radiol 2016;85(1):61-67.

18. Avery R, Kuo PH. 18F Sodium Fluoride PET/CT Detects Osseous Metastases From Breast Cancer Missed on FDG PET/CT With Marrow Rebound. Clin Nucl Med 2013;38(9):746-748.

19. Liu T, Wang S, Liu H, Meng B, Zhou F, HE F, et al. Detection of vertebral metastases: a meta-analysis comparing MRI, CT, PET, BS and BS with SPECT. J Cancer Res Clin Oncol 2017;143(3):457-465.

20. Jacobs MA, Macura KJ, Zaheer A, Antonarakis ES, Stearns V, Wolff AC, et al. Multiparametric Whole-body MRI with Diffusion-weighted Imaging and ADC Mapping for the Identification of Visceral and Osseous Metastases from Solid Tumors. Acad Radiol 2018;25(11):1405-1414.